

1 Reducing Uncertainty in Chemistry Climate Model Predictions of Stratospheric Ozone

2

3 A. R. Douglass¹, S. E. Strahan², L. D. Oman¹, R. S. Stolarski³

4

5

6

7

8 ¹NASA Goddard Space Flight Center, Greenbelt MD, USA

9 ²University Space Research Association, Columbia, MD, USA

10 ³Johns Hopkins University, Baltimore, MD, USA

11

11 **Abstract**

12 Chemistry climate models (CCMs) are used to predict the future evolution of
13 stratospheric ozone as ozone-depleting substances decrease and greenhouse gases
14 increase, cooling the stratosphere. CCM predictions exhibit many common features, but
15 also a broad range of values for quantities such as year of ozone-return-to-1980 and
16 global ozone level at the end of the 21st century. Multiple linear regression is applied to
17 each of 14 CCMs to separate ozone response to chlorine change from that due to climate
18 change. We show that the sensitivity of lower atmosphere ozone to chlorine change
19 $\Delta O_3/\Delta Cl_y$ is a near linear function of partitioning of total inorganic chlorine (Cl_y) into its
20 reservoirs; both Cl_y and its partitioning are controlled by lower atmospheric transport.
21 CCMs with realistic transport agree with observations for chlorine reservoirs and produce
22 similar ozone responses to chlorine change. After 2035 differences in $\Delta O_3/\Delta Cl_y$
23 contribute little to the spread in CCM results as the anthropogenic contribution to Cl_y
24 becomes unimportant. Differences among upper stratospheric ozone increases due to
25 temperature decreases are explained by differences in ozone sensitivity to temperature
26 change $\Delta O_3/\Delta T$ due to different contributions from various ozone loss processes, each
27 with their own temperature dependence. In the lower atmosphere, tropical ozone
28 decreases caused by a predicted speed-up in the Brewer-Dobson circulation may or may
29 not be balanced by middle and high latitude increases, contributing most to the spread in
30 late 21st century predictions.

31

32

1. Introduction

If anthropogenic ozone depleting substances (ODSs) were the only change in atmospheric composition, ozone (O_3) and stratospheric chlorine would be expected to return to unperturbed levels as ODSs were removed from the atmosphere. Other concurrent changes in composition complicate the picture, and the anticipated increases in greenhouse gases leading to stratospheric cooling and circulation changes are also expected to impact the future global ozone distribution. Stratospheric cooling causes ozone to increase by slowing temperature dependent ozone loss processes. All chemistry climate models (CCMs) predict a speed-up in the Brewer Dobson circulation, leading to a decrease in stratospheric tropical ozone column and increased ozone in middle and high latitudes, depending on the structure of the circulation change [Austin and Wilson, 2006; Shepherd, 2008; Waugh *et al.*, 2009]. In spite of commonalities in simulated ozone evolution as noted by Oman *et al.* [2010], there are significant differences in the predictions that are the subject of this work.

Eyring *et al.* [2005] describe the on-going community effort, sponsored by Stratospheric Processes and Their Role in Climate (SPARC), to evaluate CCMs (CCMVal). The CCMVal project used diagnostics developed from observations to evaluate dynamical, chemical, and radiative processes in CCMs. The CCMs, their simulations, and the results of the evaluations are described in the CCMVal report [SPARC CCMVal, 2010, hereafter referred to as CCMVal2010]. These simulations were also contributed to the World Meteorological Organization *Scientific Assessment of Ozone Depletion: 2010* [WMO, 2011; hereafter referred to as WMO2011]. Although CCMVal used observations to show

that chemical and transport processes were not well-represented by the CCMs in all cases, this information was not used to discriminate among CCMs. Predictions of 21st century ozone used in WMO2011 were obtained using a time series additive model (TSAM) method described in Chapter 9 of *CCMVal2010* and *Scinocca et al.* [2010] to produce multi-model trends (MMT). The use of such methods to combine results of simulations is widespread in science and economics, and is a better predictor than individual models when the models are independent and unbiased. The CCMs participating in CCMVal and WMO2011 are not completely independent as they share common elements such as the advection scheme or core general circulation model. Perhaps more important, the *CCMVAL2010* evaluation reveals deficiencies for some CCMs such as non-conservation of mass, missing chemical reactions, or poor representation of various processes that result in poor comparisons of constituent distributions with observations. When simulations include known and identified deficiencies, the MMT becomes less credible as the best predictor.

Waugh and Eyring [2008] compared a prediction for total column ozone (TCO) obtained using performance metrics to weight the contributions from various CCMs with an unweighted multi-model mean (MMM), and found only small differences between these weighted and unweighted predictions. Their analysis also revealed some issues with the strategy of weighting contributions to obtain a better prediction, noting that the diagnostics were not independent of each other. In addition, performance on a particular diagnostic of the present atmosphere might or might not be related to the ozone response to composition change.

Recent studies have taken a different approach to the use of diagnostics of chemistry and transport diagnostics to explain differences among simulations. *Strahan et al.* [2011] used an expanded set of transport diagnostics for the lower stratosphere to show that four CCMs with the most realistic representation of transport also produced a much narrower range of predicted TCO return-to-1980 dates than the suite of CCMs that contributed simulations to *CCMVAL2010* and *WMO2011*. These same four CCMs also had no significant errors or omissions in their chemical mechanism. *Douglass et al.* [2012] examined the upper stratospheric ozone response to chlorine and temperature. The reaction $O + O_3 \rightarrow 2 O_2$ and catalytic loss cycles involving chlorine, nitrogen and hydrogen radicals that have the same net effect control upper stratospheric ozone. The temperature dependence of the loss processes varies; $O + O_3$ is most temperature dependent and the chlorine catalytic cycle is least. *Douglass et al.* [2012] showed that the CCMs produce a wide, often unrealistic, range of upper atmospheric temperatures for the present atmosphere. Together that range and differences in constituents such as reactive nitrogen account for differences in the relative importance of the catalytic loss cycles. All of the CCMs predict increases in upper stratospheric ozone as anthropogenic chlorine and temperatures decrease in the 21st century. However, there are differences in the magnitude of increases predicted by the CCMs that become larger as anthropogenic chlorine decreases even though their predicted temperature decreases are similar because the ozone sensitivity to temperature change varies among CCMs. Neither of these studies elucidates the link between transport and lower stratospheric chemistry implied by the *Strahan et al.* [2011] result.

This paper demonstrates that many of the differences in the predicted evolution of stratospheric ozone can be interpreted and understood using a subset of CCMVal diagnostics and concepts that describe interactions among photochemical, transport and radiative processes that control stratospheric ozone. We apply multiple linear regression (MLR) to the future simulations that were used in the CCMVal exercise and *WMO2011* in order to separate contributions of chlorine change from other factors that contribute to future ozone evolution. MLR has been successfully applied to observational data sets and CCM output to quantify the ozone response to chlorine by accounting for other factors known to affect ozone levels such as volcanic injection of stratospheric aerosols, solar cycle variability and the quasi-biennial oscillation [*Stolarski et al.*, 1991; *Stolarski et al.*, 2006]. This approach was also applied to future simulations to separate the ozone response to chlorine change from that due to other changes in composition and climate [*Stolarski et al.*, 2009; *Oman et al.*, 2010]. The results of this separation will then be examined with two goals. The first is to explain the narrower range of values for the predicted year of ozone return to 1980 that is obtained from CCMs with the most realistic performance on transport diagnostics as detailed by *Strahan et al.* [2011]. This part of the analysis focuses on the simulated ozone responses to changes in ODSs. The second goal is to explain the differences in the ozone response to the ongoing changes in greenhouse gases (excluding ODSs) that lead to changes in stratospheric circulation and temperature. These differences in response cause the future simulations to diverge from one another in the middle to late 21st century.

The simulations and the CCMs that produce them are briefly described in section 2. Section 2 also describes datasets that contribute to interpretation of the simulated ozone evolution. The analysis strategy and results are presented in section 3. Section 4 describes relationships between the sensitivity of simulated ozone to chlorine change and the simulation of the present atmosphere. Section 5 considers ozone after 2035 as the anthropogenic contribution to chlorine levels decreases and the ozone response to climate change becomes dominant. Results and their implications are summarized in section 6.

2. Chemistry Climate Models, Simulations and Data

2.1 CCMVal Models and Simulations

Morgenstern et al. [2010] and *Oman et al.* [2010] present a detailed overview of the models, inputs, and scenarios used in the CCMVal-2 exercise. These models contributed simulations that are evaluated in the *CCMVAL2010* and used in *WMO2011* Chapter 2 (Stratospheric Ozone and Surface Ultraviolet Radiation [*Douglass and Fioletov et al.*, 2011]) and Chapter 3 (Future Ozone and Its Impact on Surface UV [*Bekki and Bodeker et al.*, 2011]). Eighteen groups contributed simulations to CCMVal-2, but for this analysis we include only the fourteen models that contributed a future scenario simulation and whose vertical domain includes the upper stratosphere. These models are listed in Table 1. The future scenario (referred to as REF-B2) uses the A1B greenhouse gas scenario from the Intergovernmental Panel on Climate Change (IPCC) [2000] and the revised A1 halogen scenario from *WMO* [2007] and *CCMVal2010*. Most models have simulations that cover 1960 – 2099 with 10-year model spin-up prior to 1960. The Unified

Model/United Kingdom Chemistry Aerosol Community Model – Met Office
(UMUKCA-METO) future simulation ends in 2083.

2.2 Observations

We use observations to show how the simulated distributions of reservoir gases such as hydrogen chloride (HCl) and chlorine nitrate (ClONO₂) depend on realistic lower stratospheric transport in order to establish context for discussion. We otherwise do not repeat the comprehensive evaluation of photochemistry in Chapter 6 of the *CCMVal2010* report, or identify ‘best’ simulations that agree with one or more sets of observations.

Network for the Detection of Atmospheric Composition Change

A primary goal of the Network for the Detection of Atmospheric Composition Change (NDAAC) is to obtain consistent, standardized, long-term measurements of atmospheric trace gases at a set of globally distributed research stations to detect trends in atmospheric composition. Here we consider timeseries of the total column abundances of HCl and ClONO₂ obtained using Fourier Transform Infrared Spectrometers (FTIR) from eight of the long-term measurement sites listed in Table 2. These sites were selected from the 18 FTIR locations listed in the measurements and analysis subdirectory to encompass a broad latitude range with temporal records of nine years or longer. *Rinsland et al.* [2003] discuss such measurements in detail, and show that the build-up and leveling off of the sum of HCl and ClONO₂ columns from six of these sites and others not included here is consistent with timeseries for surface source gases and with upper stratospheric HCl as measured by the Halogen Occultation Instrument on the Upper Atmosphere Research

Satellite, confirming the effectiveness of the Montreal Protocol and its amendments in reducing the anthropogenic contribution to atmospheric chlorine. Details about the measurements are provided by *Rinsland et al.* [2003] and references therein, and can also be obtained from the NDAAC website <http://www.ndacc.org/>.

SciSat Atmospheric Chemistry Experiment

The Atmospheric Chemistry Experiment (ACE) on the Canadian satellite SCI-SAT-1 is a Fourier Transform Spectrometer (FTS). ACE-FTS is a solar occultation instrument that obtains high resolution spectra (0.02 cm^{-1}) between $750\text{--}4400\text{ cm}^{-1}$ [*Bernath et al.*, 2005]. ACE-FTS makes daily measurements in each of two latitudes bands for sunrise and sunset. Vertical profiles are retrieved for up to 15 sunrises and 15 sunsets per day. Of the many species obtained by ACE-FTS, here we use V3 ClONO₂ and HCl profiles, focusing on middle latitudes between 50 and 10 hPa.

3. MLR Analyses of CCM Ozone Columns

3.1 Total column ozone time series in CCMs

Figure 1 shows the evolution of differences from 1980 for the 60°S-60°N and 90°S-90°N averages of total column ozone (TCO) simulated by the CCMVal models. The 1980 mean is approximated by a five-year average of annual means (1978-1982) to reduce the importance of year-to-year variations. The range of differences among simulations in 2100 (~ 10 DU) is substantially smaller than the range in 2000 (~ 15 DU) when the stratospheric chlorine was near its peak value. However, the simulated range of ozone loss due to chlorine change is unrealistically large compared with the estimates of ozone

depletion obtained from observations. *WMO2010* reported 60°S-60°N column ozone levels to be 3.5% (~10 DU) less than 1980. The range of simulated increases in global column ozone in 2100 relative to 1980 is comparable to the observed depletion due to anthropogenic chlorine and thus indicates significant uncertainty.

In each panel of Figure 1 the four blue traces identify the simulations from the CCMs that have the most realistic transport based on the expanded version of the tracer diagnostics used in Chapter 5 of *CCMVal2010* as reported by *Strahan et al.* [2011]. The black dashed vertical lines indicate the earliest and latest years for return-to-1980; the blue dashed vertical lines show the narrower range of return years for the CCMs with realistic transport. These ranges are nearly the same for the 60°S – 60°N and 90°S – 90°N averages. The differences from the 1980 mean are more negative around 2000 and more positive beginning ~2050 for the global average compared with the 60°S – 60°N average. The contribution from springtime lower stratosphere polar ozone loss that is included in the global average explains the more negative difference in 2000. Acceleration of the Brewer Dobson Circulation (BDC), predicted by all CCMs [*Butchart et al.*, 2006; *Butchart et al.*, 2010] causes a tropical ozone decrease that is countered by middle and high latitude ozone increases [*Li et al.*, 2009]. The high latitude average includes more of the lower stratosphere middle and high latitude ozone increase, explaining the more positive differences from 1980 after 2050 for the 90°S – 90°N averages. Because the differences among the simulations are similar for the both spatial averages, further

discussion considers only the 60°S – 60°N that was discussed by *Strahan et al.* [2011] and is commonly considered in the WMO assessments.

Figure 1 shows that the differences in CCM responses to increasing chlorine vary by ~15 DU over a 20-yr period in spite of using identical chlorine source gas boundary conditions. This suggests that the amount and distribution of stratospheric inorganic chlorine (Cl_y) in the CCMs varies, resulting in differences in the ozone response to the specified chlorine change.

In order to quantify and explain such differences in the ozone sensitivity to changes in chlorine and climate, our strategy is to analyze the output from each CCM using multiple linear regression (MLR). This method, which has been applied to observed and simulated timeseries [*Stolarski et al.*, 1991; *Stolarski et al.*, 2009] capitalizes on the length of the simulated time series to separate the contributions of chlorine change and climate change (i.e., circulation and temperature) to ozone evolution. For each CCM the timeseries used in the MLR begins in 1960 and extends to 2083 for the shortest simulation and to within one or two years of 2100 for the others.

We explored several options for explanatory variables in the MLR. The chlorine change is always represented by equivalent effective stratospheric chlorine (EESC) [*Newman et al.*, 2007]. Circulation or climate-related changes are represented by timeseries of monthly mean vertical velocities at 70 hPa averaged for 20°S – 20°N or the normalized timeseries of lower tropical stratosphere gradients in long-lived tracers such as N_2O or

CFC1₃. In practice, any of these choices is equivalent to a combination of EESC, a linear trend and the time dependence of the change in upwelling (for the few cases where this change is not linear). All options produce similar values for the ozone sensitivities to chlorine change and climate change (including both changes in temperature and circulation) within each CCM. Examples are shown in Figure 2. In each panel, the crosses are the annual average ozone between 60°S and 60°N from a particular CCM. The black solid line is the fit to the simulation obtained from MLR. The green line is the mean value plus the contribution to the temporal evolution due to chlorine change; the blue line is the mean value plus the contribution due to changes in climate. The fits obtained from the MLR capture the time dependence of each simulation. MLR fitting facilitates comparisons among CCMs by reducing noise due to interannual variability when computing ozone differences for various time periods.

In all of the CCMs, most of the change in TCO from 1980-2000 is due to chlorine change. For the ensemble of simulations the mean and standard deviation of the ozone decrease between 1980 and 2000 attributed to chlorine increase are -9.4 DU and 4.0 DU. The mean and standard deviation of the ensemble of ozone change due to climate change are 0.8 DU and 0.7 DU, respectively. For the examples in Figure 2 the 60°S-60°N ozone change between 1980 and 2000 due to climate changes is ~1.25 DU. In contrast, the 60°S-60°N ozone changes due to chlorine increase are -8.4 DU and -18.4 DU.

3.2 Ozone Response in the Upper Stratosphere and Lower Atmosphere

258 Projected changes in greenhouse gases (GHG) and ODSs will have different impacts on
259 the upper and lower stratospheric ozone because the ozone response to these composition
260 changes varies because the timescales for processes controlling ozone vary with height.
261 In the upper stratosphere, fast radical photochemistry controls the ozone level on
262 timescales of days, while transport controls O₃ on seasonal to multi-decadal timescales
263 through the slowly changing levels of long-lived source gases and reservoir species that
264 control the levels of total reactive nitrogen (NO_y) and Cl_y. In the lower stratosphere
265 where ozone is long-lived, the chemical and transport processes have similar timescales.
266 The predicted speed-up in the Brewer Dobson circulation will affect processes
267 controlling ozone at all timescales through its effects on composition, chemistry,
268 transport, and temperature..

269

270 In addition to its application to the total column ozone as discussed in the previous
271 section, here we use MLR to quantify the effects of GHG and ODS changes on ozone in
272 two partial columns: the upper troposphere and the mid-stratosphere (500 hPa – 20 hPa),
273 hereinafter referred to as the lower atmosphere (LA), and the upper stratosphere (US) (20
274 hPa – 1 hPa). As for the TCO, MLR is applied to timeseries from 1980 to the final
275 simulated year for each CCM. Ozone changes are computed from the resulting MLR fits
276 for time periods when changes in chlorine loading are large (1980-2000) and when they
277 are small (1980-2035). The TCO differences and the contributions from the upper
278 stratosphere and lower atmosphere columns are shown for each CCM in Figure 3. The
279 year 2035 is chosen because it is near the midpoint of the range of return years (2026 –
280 2040) for the CCMs with realistic transport identified by *Strahan et al.* [2011] and also

because chlorine change and climate change make similar contributions to the differences in projections as will be discussed in the following section.

Figure 3a shows that while chlorine loading is increasing (1980-2000), ozone changes are negative in both the LA and US columns in most CCMs. The TCO changes among the CCMs range from -3 to -17 DU; most of this variance comes from the LA response. For the ozone change between 2035 and 1980 (Figure 3b), the LA changes are negative in most CCMs whereas the US changes are positive or less than -0.7 DU. The TCO change can be positive (beyond ‘recovery’), near zero (‘recovery’), or negative (not yet ‘recovered’). The range of predicted TCO difference for 2035-1980 (standard deviation 2.6 DU) is less than that predicted for 2000-1980 (standard deviation 4.1 DU). The LA changes in this period again contribute the most to the differences among predictions.

3.3 Contributions of Chlorine and Climate Change to Ozone Response

3.3.1 Total Column Ozone Changes

In Figure 4 we separate the chlorine and climate change contributions to the TCO change to explain the variance among CCMs shown in Fig. 3b. Ten CCMs, including the four with the most realistic transport, are clustered near the vertical dashed line, showing the balance between the contributions of chlorine change and climate change among these CCMs that are close to 1980 O₃ levels by 2035. Among these CCMs, the TCO change between 1980 and 2035 is most negative for those with the smallest increase due to climate change. Three of the CCMs that are 4 or more DU from their 1980 value are among those with the greatest change due to chlorine; two of these three have negative

ozone response due to climate change. The CCM with the earliest recovery (more than 2.5 DU greater than 1980 in 2035) has weak sensitivity to chlorine change and the most positive response to climate change.

3.3.2 *Separation of Processes Affecting Lower and Upper Ozone Columns*

From 1980 to 2000, the correlation between upper and lower column ozone responses is 0.6; this is not surprising since chlorine related processes dominate the loss in both regions. The correlation gradually declines to 0.2 between 2000 and 2050, as atmospheric chlorine decreases and the contributions from climate change increase. This shows that different mechanisms control the ozone response during different time periods and that upper and lower atmosphere responses of ozone to climate change are not correlated. This prompts separate investigation of the processes contributing to upper and lower column ozone change from 1980.

Douglass et al. [2012] show that upper stratospheric ozone levels prior to 1980 are higher for the CCMs with colder upper atmospheres and vice versa. They use the framework developed by *Stolarski and Douglass* [1985] to explain how differences in unperturbed values for ozone level, temperature and reactive nitrogen contribute to differences in sensitivity of ozone to perturbations in temperature and chlorine. The amplitude of the temperature-dependent annual cycle in ozone varies as expected, decreasing as chlorine increases in all CCMs because the chlorine catalyzed loss cycle is less dependent on temperature. In the LA both photochemical and transport terms are important. Chlorine change has a small impact on the ozone response to temperature change. In this section,

we use MLR to separate the ozone change related to chlorine from other processes in the LA and US, presenting results for two time periods.

Figure 5a shows the simulated ozone changes in the LA from 1980-2000. The response due to chlorine increase (green diamonds) greatly exceeds the ozone change due to climate change (blue triangles) in all but one of the CCMs. In addition, ozone response to increased chlorine contributes much more to inter-model differences than the response to climate change (4.3 DU and 0.6 DU standard deviations, respectively). In comparison, the lower atmosphere ozone difference between 1980 and 2035 due to chlorine is less than half the difference between 1980 and 2000 and there is also less variance among CCMs (Figure 5b). By 2035 middle latitude lower stratospheric inorganic chlorine has decreased by 20-40% from its peak value, depending on the pressure level and CCM being examined, explaining to the smaller contribution from chlorine related processes. The differences among the climate change responses between 2035 and 1980 are larger than those for chlorine.

US changes between 1980 and 2000 (Figure 5c) are broadly similar to the LA but exhibit significantly less model-to-model variability (Figure 5a). The ozone change due to chlorine increase dominates the overall response, and differences in sensitivity to chlorine change contribute to the variability among CCMs. The ozone response to climate change is positive and about 1.1 DU in all CCMs. By 2035 (Figure 5d), the ozone change due to chlorine change has decreased while the O₃ increase due to climate change has increased; this increase is both larger and more variable than the ozone decrease due to chlorine.

Douglass et al. [2012] show that temperature changes are comparable among CCMs, thus the differences in ozone response to climate change reflect differences in ozone sensitivity to temperature. Ozone sensitivity to climate change is similar among CCMs in 2000 and different in 2035. This is expected because when ozone loss due to chlorine is a larger fraction of all losses, as in 2000, O₃ is less sensitive to temperature change because the chlorine loss reaction is the least temperature dependent of all the loss processes.

Figure 6 shows how the standard deviation among the 14 simulations of the 60°S-60°N TCO differences from 1980 changes between 1980 and 2080, separating the contributions from chlorine change (green) and climate change (blue). Until about 2000, the differences in ozone sensitivity to chlorine change account for nearly all of the variation among CCM predictions. The contribution from climate change rises throughout the integration, equaling the contribution from chlorine change in about 2035. The chlorine contribution to inter-model differences continues to decline as expected as chlorine declines, while the contribution of climate change continues to increase. By 2080, the differences in chlorine sensitivity do not contribute significantly to inter-model differences, and the climate change contribution is ~70% of the magnitude of the peak chlorine contribution in 2005.

4. Explaining differences in ozone projections

Figure 1 shows that in 2000 the range of CCM values for the difference from 1980 for 60°S-60°N or 90°S-90°N TCO amounts is approximately 15 DU. By about 2080, the

range is about 9 DU and the contribution of the simulated ozone response to stratospheric chlorine change is near zero (Figure 6). The MLR analysis presented in the previous section, summarized by Figure 6, shows that understanding the differences among CCM predictions requires understanding both the differences in ozone sensitivity to chlorine and the differences in ozone sensitivity to climate change, especially in the LA. To explain the narrower range for TCO return to 1980 for CCMs with most realistic transport, we demonstrate the relationship between transport and lower stratosphere distributions of chlorine reservoirs, linking those distributions with the simulated sensitivity of LA ozone to chlorine change.

All CCMs solve a continuity equation for the ozone mixing ratio γ_{O_3} at each grid point that includes chemical production (P), loss (L) and transport terms:

$$\frac{\partial \gamma_{O_3}}{\partial t} = P - L + transport$$

Below about 50 km ozone is very nearly equal to the sum of ozone and atomic oxygen, and photolysis of ozone producing atomic oxygen and reformation of ozone through reaction of atomic and molecular oxygen are in approximate balance. Production is mainly photolysis of molecular oxygen producing two oxygen atoms that form ozone molecules by reaction of atomic and molecular oxygen. In addition to the reaction of atomic oxygen with ozone, catalytic cycles involving hydrogen, nitrogen and chlorine radicals contribute to ozone loss.

As atmospheric composition changes, realistic computation of the $\partial\gamma_{O_3}/\partial t$ requires appropriate contributions from the photochemical and transport terms. A realistic estimate of the fractional change in L requires realistic representation of the fractional importance of each catalytic cycle to the total loss in an unperturbed atmosphere. Short-lived radicals (e.g., chlorine monoxide (ClO), hydroxyl (OH) and nitrogen dioxide (NO₂)) participate in catalytic ozone loss. Although radicals are short-lived, transport processes affect ozone loss through their influence on the distributions of long-lived gases and reservoir gases. Source gases such as chlorofluorocarbons and nitrous oxide (N₂O) produce radicals when destroyed in the stratosphere, Reservoir gases such as hydrogen chloride (HCl) and chlorine nitrate (ClONO₂) are produced by reactions of radicals with source gases or with each other. *Dessler et al.* [1995] showed that the partitioning between ClONO₂ and HCl as observed by instruments on the Upper Atmosphere Research Satellite (UARS) follows expectation; the ratio ClONO₂/HCl is quadratically dependent on ozone, linearly dependent on the hydroxyl radical and inversely dependent on methane. In the lower stratosphere the distributions of both ozone and methane are strongly influenced by transport. *Dessler et al.* [1996] showed the broad agreement between observed and expected partitioning of the reservoir ClONO₂ and the radical chlorine monoxide using UARS observations of ClO, NO₂ and ClONO₂ along with laboratory data. Thus, the influence of transport on radical distributions in the lower stratosphere causes higher levels of ClONO₂ to produce higher levels of ClO. Such simulations will have greater contributions of chlorine-catalyzed loss to the ozone tendency.

Chapter 6 of *CCMVal2010* compared timeseries of HCl and ClONO₂ at the Jungfraujoch station (46.6°N) with timeseries simulated by CCMs; these are likely indicators of the simulated lower atmosphere sensitivity to chlorine because for both species more than 70% of the total column resides below 20 hPa. The simulated HCl columns shown in Figure 7 span a wide range of values, with peak annual mean values between 3.1×10^{15} and 6.4×10^{15} molecules/cm² (disregarding one CCM with an extremely high peak value due to lack of tropospheric rainout of HCl) compared with 4.0×10^{15} , the 1998 – 2001 average of HCl column measurements at Jungfraujoch. The simulated columns generally exhibit the observed time dependence because the time dependence of the chlorine containing source gases (e.g., CFCI₃ and CF₂Cl₂) is controlled by the boundary conditions. The Cl_y produced by destruction of these molecules varies substantially among the CCMs, and differences in Cl_y and its partitioning between the chlorine reservoirs both contribute to the large spread in computed values of the HCl columns.

The link between transport and gas phase photochemistry in the lower stratosphere is demonstrated by comparisons of observed and simulated HCl columns in Figure 7. We use seven stations that span 68°N-45°S (Table 2) but are outside the polar vortices, avoiding large seasonal variations in their columns [*Santee et al.*, 2008]. The right column compares the subset of CCMs with realistic transport identified by *Strahan et al.* [2011] with observed HCl columns; the left column compares timeseries from the remaining CCMs. For the entire latitude range, observed and simulated HCl columns are in much better agreement for simulations that perform well on transport diagnostics. Because observations are made at irregular intervals throughout the year, the CCM

monthly zonal means are compared with daily measurements from each station. Observed variability neither zonally nor monthly averaged, like the CCMs, and so appears much larger.

We further investigate the partitioning between HCl and ClONO₂ reservoirs using observations from the ACE-FTS. Figure 8a shows profiles from the 14 CCMs of ClONO₂/Cl_y (\approx ClONO₂/(ClONO₂ + HCl for 20 hPa and higher pressures in winter) for December 2005. Blue lines indicate the four with most realistic transport, black lines are the others. The red line indicates the December mean of ACE-FTS profiles between 40°N-50°N, 50 hPa – 20 hPa; horizontal lines are the standard deviation of the observed profiles. The CCM with the highest values for ClONO₂/Cl_y has a known error in the photochemical mechanism that leads to lower HCl.

Figure 5 shows that the contribution of chlorine processes to lower atmospheric ozone column change between 2000 and 1980 varies substantially among CCMs. Much of the variation in response is explained by the partitioning of chlorine reservoirs shown in Figure 8b. The sensitivity of lower atmosphere ozone to chlorine change ($\Delta O_3/\Delta Cl_y$) obtained from the MLR is shown as a function of the simulated partitioning of the chlorine reservoirs ($ClONO_2/Cl_y \approx ClONO_2/(ClONO_2+HCl)$) at 45°N for December 2005 in Figure 8b. The symbol color indicates the total chlorine level at 20 hPa, and the range of values from ACE-FTS for December 2005, 40°N-50°N is shown on the color bar. The three CCMs that are least sensitive to chlorine change have lower than observed values of ClONO₂/Cl_y, and also higher than observed values for total Cl_y. The simulations that are

most sensitive to chlorine have higher than observed levels of $\text{ClONO}_2/\text{Cl}_y$. The sensitivity $\Delta O_3/\Delta \text{Cl}_y$ is negatively correlated with $\text{ClONO}_2/\text{Cl}_y$ between 50 and 10 hPa for all months. The correlation reaches its maximum value between 30 and 20 hPa (the peak for $\text{ClONO}_2/\text{Cl}_y$) during winter months, and is -0.78 at 20 hPa in December. Note that observations and simulations confirm that for this pressure range distributions of reservoirs control the radical distributions [Dessler *et al.* 1996]. Stolarski and Douglass [1986] and Douglass and Stolarski [1987] used a one-dimensional model to show larger (smaller) ozone sensitivity to chlorine change for higher (lower) levels of chlorine radicals in the “present” simulated lower atmosphere. The CCMs investigated here produce the same result. Simulations with higher levels of chlorine radicals inferred by partitioning of reservoirs are more sensitive to chlorine change and vice-versa. The transport diagnostics select CCMs with similar Cl_y levels in the lower stratosphere and similar partitioning of reservoirs, implying similar contributions of chlorine catalyzed loss processes to ozone loss. The Cl_y levels and partitioning of reservoirs for the CCMs with most realistic transport also agree with the NDACC columns and the observations from ACE-FTS. This result and the similar TCO increases due to climate change shown in Figure 5 explain narrower range for year-of-return-to-1980 for CCMs with realistic performance on transport diagnostics discussed by Strahan *et al.* [2011].

As chlorine decreases, the chlorine contribution to the total change in ozone decreases and differences in chlorine reservoir distributions caused by differences in lower stratospheric transport contribute less to the variance in simulated ozone. Figure 6

shows that after 2035 the differences in the response to climate change make the larger contribution to the spread among the CCM predictions.

5. Stratospheric ozone after 2035

The contributions to ozone change for 2080 – 1980 from chlorine change and from climate change are compared in Figure 9. Although the anthropogenic contribution to Cl_y is not zero, the Cl_y level in 2080 is less than the 1980 level, and the annually averaged 60°S to 60°N total column ozone change relative to 1980 due to chlorine change is always positive, falling between 0.5 and 2.2 DU (Figure 9a). The ozone change due to chlorine change is always positive in the upper stratosphere and is positive in the lower stratosphere with one exception because for all but one CCM the anthropogenic contribution to stratospheric chlorine is smaller in 2080 than in 1980. Chlorine plays a small role compared with climate change, as shown in Figure 9b (note different scales for the y-axis).

Climate change affects ozone through cooling and through changes in circulation. All CCMs predict a speedup in the Brewer Dobson circulation, leading to ozone decreases in the tropical lower stratosphere and increases at middle and high latitudes. Stratospheric cooling results in slower rates of ozone loss processes, producing increased ozone. Twelve of the CCMs produce a net ozone increase relative to their 1980 level by 2060 as impact of chlorine change decreases. The maximum predicted increase for 2080 relative to 1980 due to processes related to climate change is more than 8 DU.

The changes in TCO and the separate contributions from the upper stratosphere and lower atmosphere due to climate related processes are shown in Figure 9b. The standard deviation of the total column ozone increase due to climate change (~3DU) is comparable to the multi-model mean increase (~4DU). This large variance is caused by a bimodal distribution in model differences between the US and LA columns. In the US, the CCMs consistently produce an ozone increase. In the LA, seven of the CCMs predict a contribution of less than 1 DU. For these CCMs the TCO response to climate change is controlled by the US. The mean TCO increase for these seven CCMs is about 5.6 DU, with a standard deviation of 1.2 DU. *Li et al.* [2009] discuss near the cancellation of tropical and extratropical LA ozone changes in the GEOSCCM that leads to a small net LA response to climate change, and show that the TCO increase due to climate change is approximately equal to the increase in the US. In six of the CCMs the LA ozone decrease due to increased tropical upwelling exceeds extratropical increases such that the latitudinally averaged response to climate change is negative. In these six CCMs the LA ozone decrease is opposed by the US increase; mean TCO response is smaller (2.3 DU) but the standard deviation is larger (3.6 DU) compared with the seven CCMs with small contributions from the LA. In one CCM the extratropical increases exceed the tropical decrease; the LA and US increases combine to produce the TCO increase of more than 8 DU.

Although complete information is not available for these fourteen CCMs, this difference in the net lower atmospheric ozone response appears to be linked to differences in the simulated increases in upwelling. For example, Figure 4.11 in *CCMVal2010* shows that

the 9 CCMs producing timeseries longer than 100 years fall into two groups. The annual mean upward mass flux at 70 hPa as calculated from w^* for a ‘high’ group containing 5 CCMs shows increases from a 1960 value $\sim 5.8 \times 10^9$ kg/s to values as high as $7\text{--}9.2 \times 10^9$ kg/s. In contrast, the annual mean upward mass flux at 70 hPa for a ‘low’ group containing 4 CCMs is initially $\sim 4.8 \times 10^9$ kg/s and increases to $6\text{--}6.5 \times 10^9$ kg/s. The simulations considered here also included in *CCMVal2010* Figure 4.11 separate into two groups based largely on the change in mass flux. The CCMs in the ‘high’ group all produce substantial net lower stratospheric ozone decreases due to climate change; the CCMs in the ‘low’ group all produce more complete cancellation.

Although the US and LA both contribute to the range of CCM responses; the range of US responses is smaller than that of the LA. *Douglass et al.* [2012] considered the US response in detail, showing that differences in the UA response to temperature change are partially explained by the simulated ozone levels themselves. CCMs that produce higher (lower) ozone levels for the 1960–1980 timeframe are more (less) sensitive to temperature change because the most temperature dependent loss process $O + O_3$ contributes more (less) to the net ozone loss. Although this is not the only factor that affects the simulated response, this approach does give insight into the responses of the outliers. The CCM that produces the largest US ozone response to climate change (> 8 DU) also produces the largest unperturbed US ozone partial column, exceeding the multi-model mean by more than 15%. In contrast, the CCM that produces the smallest upper stratospheric response to climate change (< 3 DU) produces an unperturbed US partial ozone column that is about 15% less than the multimodel mean.

To summarize, compensation or lack thereof between the LA decrease in tropical ozone and middle and high latitude LA increase contributes much to the range of responses, but whether or not such compensation is produced is not related to performance on transport diagnostics. Figure 1 shows that the CCMs identified with best performance on transport diagnostics separate after about 2050, with predictions of ozone increases for 2 CCMs each at the high and low ends of the range for the 14 CCMs. For the CCMs included in Figure 4.11 of *SPARCCCMVAL*, the high and low predictions of ozone change are consistent with the CCM falling in the group with high change in mass flux (larger LA decrease opposing US increase resulting in smaller TCO increase) and low change in mass flux (more cancellation between tropical and extra-tropical LA ozone changes and larger total column increase).

The response of the circulation to climate change is robust among the CCMs in the sense that all CCMs predict an increase of tropical upwelling, however the response is less than robust in two ways. First, the rate of increase varies, and in some of the CCMs the appearance and disappearance of the ozone hole affects the rate of increase. For example, *Li et al.* [2009] show that in the GEOSCCM the rate of increase is about 1/3 faster during the formation phase of the ozone hole and 1/3 slower as the ozone hole dissipates compared with the rate of increase in the late 2000's when chlorine change ceases to be significant. Note that GEOSCCM is in the group with 'low' change in annual mean upward mass flux at 70 hPa. Analysis of the time dependence of the annual mean upwelling for the subset of CCMs that provide timeseries of w^* shows that the rate of increase may be faster, slower or unaffected by ozone hole formation and dissipation.

Second, the extratropical circulation changes and their convolution with simulated lower stratospheric ozone vary substantially. There are differences in both the tropical decrease and in the extratropical increase that result in near cancellation or lack thereof. Both of these factors contribute to the differences among CCM predictions for 21st century ozone.

6. Conclusions

This work quantifies the ozone response to changes in chlorine containing source gases and changing climate (i.e., stratospheric cooling and circulation change) in 14 CCMs that participated in CCMVal and contributed simulations to *WMO2010*. All models used the same time-dependent mixing ratio boundary conditions for source gases from 1960-2100. In 2035, ozone decreases relative to 1980 due to chlorine in all CCMs, since chlorine is still substantially elevated compared with 1980. The response to climate change is generally but not always positive. The 60°S-60°N annual mean ozone is within 2 DU of 1980 levels (i.e., $\Delta\text{TCO} < 1\%$) for ten of the CCMs by 2035.

Strahan et al. [2011] showed a narrower range of recovery dates for the CCMs with best performance on the CCMVal transport diagnostics compared with the range for the entire group. This work shows that differences in the sensitivity to chlorine change make the larger contribution to the spread in years for return-to-1980. These differences in chlorine sensitivity are explained by differences in the middle latitude lower stratospheric columns of chlorine reservoirs and differences in partitioning between HCl and ClONO₂. The transport diagnostics narrow the range of responses because they select CCMs with a much narrower and more realistic range of column values and partitioning among

chlorine reservoirs than produced by the suite of CCMs. By 2035 12 of 14 CCMs show an ozone increase due to climate change that is between 1 and 4 DU. The CCMs with latest recovery are either more sensitive to chlorine change or less sensitive to climate change than the CCMs identified as having most realistic transport. The CCM with much earlier recovery is least sensitive to chlorine change and among the most sensitive to climate change.

We emphasize the value of the comparisons with NDACC column measurements of the chlorine reservoirs along with comparisons of partitioning among chlorine reservoirs obtained from ACE ClONO₂ and HCl profiles, as these comparisons provide a mechanism to explain the variation in the sensitivity to chlorine change by linking lower stratospheric transport with chemistry through the control of the distributions of chlorine reservoir species. CCMs that are most sensitive to chlorine have higher values for ClONO₂/Cl_y. The column amounts of HCl and ClONO₂ depend both on total Cl_y in the lower atmosphere and its partitioning between the chlorine reservoirs. Because of the mixing ratio boundary conditions, stratospheric Cl_y can vary widely depending on the simulated transport. However, even CCMs with the most lower-atmospheric chlorine need not be the most sensitive to chlorine change, if they partition chlorine reservoirs towards HCl at the expense of ClONO₂. The ozone response to chlorine change depends on reactions with short-lived radical species; their levels are controlled by both the total Cl_y and its partitioning between the reservoir species HCl and ClONO₂.

623 In 2035, the simulated response to climate change is similar for the CCMs with most
624 realistic transport; for 12 of the 14 CCMs the response to climate change is positive and
625 between 1 and 4.5 DU. As the simulations continue, differences in the ozone response to
626 changes in circulation and temperature grow. In the US the 60°S-60°N annual average
627 ozone increases in all CCMs, and the differences in the magnitude of the increase are
628 explained by differences in the importance of the various catalytic loss cycles, such that
629 simulations with highest ozone in the unperturbed (low chlorine) period (~1960 – ~1980)
630 are most sensitive to temperature change [Douglass *et al.*, 2012]. These differences
631 account for about one third of the spread in predictions. The LA ozone response is more
632 complicated, as both circulation change and temperature change contribute. Although the
633 CCMs all predict increased upwelling, the rate of increase varies among CCMs. *Li et al.*
634 [2009] show a much larger rate of increase in w^* during ozone hole formation than
635 during ozone hole dissipation for GEOSCCM. There is no consensus among CCMs as to
636 the impact of the ozone hole on the rate of increase of w^* . *Li et al.* [2009] also note LA
637 cancellation of the impacts of the speedup of the Brewer Dobson Circulation between
638 tropical and extratropical latitudes, i.e., the tropical ozone decrease that accompanies
639 upwelling increase is opposed by middle and high latitude ozone increase. Seven of the
640 14 CCMs (including GEOSCCM) behave in a similar manner, and the net LA change due
641 to climate change for this subgroup is less than 1 DU for 2080 relative to 1980. For six
642 of the CCMs the LA impact due to climate change is substantially negative, and for one
643 the net LA impact due to climate change is substantially positive. These differences
644 contribute most to the differences in projections in the late 21st century. The CCMVal
645 diagnostics do not discriminate among the projections for w^* or the cancellation between

tropical and extratropical response. Reduction of the spread among predictions for future ozone levels requires further investigation in the differences in the response of the Brewer Dobson Circulation to increasing GHGs.

This analysis shows that the differences in projections for ozone can be explained. The US responses would be similar if the catalytic loss cycles were represented in the same balance; therefore it is important to use observations to assure that the loss cycles are represented in the appropriate balance in order to identify the ‘best’ prediction [e.g., *Douglass et al.*, 2011]. Similarly, the near linear dependence of the ozone sensitivity to chlorine on the partitioning between ClONO_2 and HCl suggest that LA responses to chlorine change will be similar if the reservoir distributions are similar, therefore it is important to use observations such as NDACC columns and profiles from ACE-FTS to assure that the reservoir distributions are realistic. In this case, deficiencies in transport relate directly to differences in the simulated response to composition change. The lower stratospheric ozone evolution is simple to diagnose given the evolution of w^* . Although it is not possible at this time to explain differences among simulations for w^* , it is likely that, as data records lengthen, analysis of observations in the tropics will make provide limits for the rate of change of w^* using such quantities as the lower stratospheric ozone or the amplitude of the quasi-biennial oscillation [*Randel and Thompson*, 2011; *Kawatani and Hamilton*, 2013].

Finally, these results, in particular linking transport diagnostics, unrealistic reservoir distributions and differences in sensitivity of simulated lower atmospheric ozone to

chlorine change, question the value of the use of a multi-model mean as a best prediction of 21st century ozone. Differences in simulated responses that can be traced to biases and understood are clearly not random. This study has identified the causes for differences in CCM ozone projections and explained the differences in lower atmosphere sensitivity to chlorine change. This work demonstrates that diagnostics used to evaluate CCM performance are most useful when they are linked with a mechanism that is related to a model's response to a perturbation. The use of such diagnostics supports a strategy to reduce uncertainty in prediction.

Acknowledgements

We acknowledge the modeling groups for making their simulations available for this analysis. The Chemistry-Climate Model Validation Activity (CCMVal) for WCRP's (World Climate research Programme) SPARC (Stratospheric Processes and their Role in Climate) project for organizing and coordinating the model data analysis activity, and the British Atmospheric Data Center (BADC) for collecting and archiving the CCMVal model output.

The data used in this publication were obtained as part of the Network for the Detection of Atmospheric Composition Change (NDACC) and are publicly available (see <http://www.ndacc.org>).

692

693

694

REFERENCES

- Akiyoshi, H., L. B. Zhou, Y. Yamashita, K. Sakamoto, M. Yoshiki, T. Nagashima, M. Takahashi, J. Kurokawa, M. Takigawa, and T. Imamura (2009), A CCM simulation of the breakup of the Antarctic polar vortex in the years 1980–2004 under the CCMVal scenarios, *J. Geophys. Res.*, *114*, D03103, doi:10.1029/2007JD009261.
- Austin, J., and R. J. Wilson (2006), Ensemble simulations of the decline and recovery of stratospheric ozone, *J. Geophys. Res.*, *111*, D16314, doi:10.1029/2005JD006907.
- Bekki, S. and G. E. Bodeker (Coordinating Lead Authors) et al. (2011), Future ozone and its impact on surface UV, Chapter 3 in *Scientific Assessment of Ozone Depletion: 2010*, Global Ozone Research and Monitoring Project – Report No. 52, 516 pp., World Meteorological Organization, Geneva, Switzerland.
- Bernath, P. F., et al. (2005), Atmospheric Chemistry Experiment (ACE): Mission overview, *Geophys. Res. Lett.*, *32*, L15S01, doi:10.1029/2005GL022386.
- Butchart N., et al. (2006), Simulations of anthropogenic change in the strength of the Brewer–Dobson circulation, *Clim. Dyn.* *27*, 727–741.
- Butchart, N., et al. (2010), Chemistry–Climate Model Simulations of Twenty-First Century Stratospheric Climate and Circulation Changes, *J. Clim.*, *23*, 5349–5373.
- Davies, T., M. J. P. Cullen, A. J. Malcolm, M. H. Mawson, A. Staniforth, A. A. White, and N. Wood (2005), A new dynamical core for the Met Office’s global and regional modelling of the atmosphere, *Q. J. R. Meteorol. Soc.*, *131*, 1759–1782, doi:10.1256/qj.04.101.

716 Déqué, M. (2007), Frequency of precipitation and temperature extremes over France in
 717 an anthropogenic scenario: Model results and statistical correction according to
 718 observed values, *Global Planet. Change*, 57, 16–26,
 719 doi:10.1016/j.gloplacha.2006.11.030.

720 de Grandpré, J., S. R. Beagley, V. I. Fomichev, E. Griffioen, J. C. McConnell, A. S.
 721 Medvedev, and T. G. Shepherd (2000), Ozone climatology using interactive
 722 chemistry: Results from the Canadian Middle Atmosphere Model, *J. Geophys.*
 723 *Res.*, 105, 26,475–26,491, doi:10.1029/ 2000JD900427.

724 Dessler, A. E., et al. (1995), Correlated observations of HCl and ClONO₂ fro UARS and
 725 implications for stratospheric chlorine partitioning, *Geophys. Res. Lett.*, 22, 1721-
 726 1724.

727 Dessler, A. E., R. Kawa, A. Douglass, D. Considine, J. Kumer, J. Waters, J. Gille (1996),
 728 A Test of the Partitioning Between ClO and ClONO₂ Based on Simultaneous
 729 UARS Measurements of ClO, NO₂, and ClONO₂, *J. Geophys. Res.*, 101, 12,515-
 730 12,521.

731 Douglass, A. R., and R. S. Stolarski, The use of atmospheric measurements to constrain
 732 model predictions of ozone change from chlorine perturbations, *J. Geophys. Res.*,
 733 92, 6662-6674, 1987.

734 Douglass, A. R. and V. Fioletov (Coordinating Lead Authors), S. Godin-Beekman, R.
 735 Müller, R. S. Stolarski, and A. Webb (2011), Stratospheric Ozone and Surface
 736 Ultraviolet Radiation, Chapter 2 in *Scientific Assessment of Ozone Depletion:*
 737 *2010*, Global Ozone Research and Monitoring Project Report No. 52, World
 738 Meteorological Organization, Geneva, Switzerland.

739 Douglass, A. R., R. S. Stolarski, S. E. Strahan, and L. D. Oman (2012), Understanding
 740 differences in upper stratospheric ozone response to changes in chlorine and
 741 temperature as computed using CCMVal-2 models, *J. Geophys. Res.*, *117*,
 742 D16306, doi:10.1029/2012JD017483
 743 Eyring, V., et al. (2005), A strategy for process-oriented validation of coupled chemistry-
 744 climate models, *Bull. Am. Meteorol. Soc.*, *86*, 1117-1133.
 745 Garcia, R. R., D. Marsh, D. E. Kinnison, B. Boville, and F. Sassi (2007), Simulations of
 746 secular trends in the middle atmosphere, 1950–2003, *J. Geophys. Res.*, *112*,
 747 D09301, doi:10.1029/2006JD007485.
 748 IPCC (Intergovernmental Panel on Climate Change) (2000), *Special Report on Emissions*
 749 *Scenarios: A Special Report of Working Group III of the Intergovernmental Panel*
 750 *on Climate Change*, 599 pp., Cambridge Univ. Press, Cambridge, U. K.
 751 Jourdain, L., S. Bekki, F. Lott and F. Lefevre (2008), The coupled chemistry-climate
 752 model LMDZ-REPROBUS: Description and evaluation of a transient simulation
 753 of the period 1980 – 1999, *Ann. Geophys.*, *26*, 1391-1413, doi:10.5194/angeo-26-
 754 1391-2008.
 755 Kawatani, Y., and K. Hamilton (2013), Weakened stratospheric quasibiennial oscillation
 756 driven by increased tropical mean upwelling, *Nature*, *497*, 478-
 757 482, doi:10.1038/nature12140.
 758 Li, F., R. S. Stolarski and P. A. Newman (2009), Stratospheric ozone in the post-CFC
 759 era, *Atmos. Chem. Phys.*, *9*, 2207–2213, doi:10.5194/acp-9-2207-2009.
 760 Morgenstern, O., P. Braesicke, F. M. O’Connor, A. C. Bushell, C. E. Johnson, S. M.
 761 Osprey, and J. A. Pyle (2009), Evaluation of the new UKCA climate composition

762 model. Part 1: The stratosphere, *Geosci. Model Dev.*, 2, 43–57, doi:10.5194/gmd-
763 2-43-2009.

764 Morgenstern, O., et al. (2010), Review of the formulation of present generation
765 stratospheric chemistry-climate models and associated external forcings, *J.*
766 *Geophys. Res.*, 115, D00M02, doi:10.1029/2009JD013728.

767 Newman, P. A., J. Daniel, D. Waugh, and E. Nash (2007), A new formulation of
768 equivalent effective stratospheric chlorine (EESC), *Atmos. Chem. Phys.*, 7, 4537–
769 4552.

770 Oman, L. D., et al. (2010), Multimodel assessment of the factors driving stratospheric
771 ozone evolution over the 21st century, *J. Geophys. Res.*, 115, D24306,
772 doi:10.1029/2010JD014362.

773 Pawson, S., R. S. Stolarski, A. R. Douglass, P. A. Newman, J. E. Nielsen, S. M. Frith,
774 and M. L. Gupta (2008), Goddard Earth Observing System chemistry-climate
775 model simulations of stratospheric ozone-temperature between 1950 and 2005, *J.*
776 *Geophys. Res.*, 113, D12103, doi:10.1029/2007JD009511.

777 Pitari, G., E. Mancini, V. Rizi, and D. T. Shindell (2002), Impact of future climate and
778 emission changes on stratospheric aerosols and ozone, *J. Atmos. Sci.*, 59, 414–
779 440, doi:10.1175/1520-0469.

780 Randel, W. J., and A. M. Thompson (2011), Interannual variability and trends in tropical
781 ozone derived from SAGE II satellite data and SHADOZ ozonesondes, *J.*
782 *Geophys. Res.*, 116, D07303, doi:10.1029/2010JD015195.

783 Rinsland, C. P., et al. (2003) Long-term trends of inorganic chlorine from ground-based
 784 infrared solar spectra: Past increases and evidence for stabilization, *J. Geophys.*
 785 *Res.*, *108*, doi:10.1029/2002JD003001.

786 Santee, M. L., I. A. MacKenzie, G. L. Manney, M. P. Chipperfield, P. F. Bernath, K. A.
 787 Walker, C. D. Boone, L. Froidevaux, N. J. Livesey, and J. W. Waters (2008), A
 788 study of stratospheric chlorine partitioning based on new satellite measurements
 789 and modeling, *J. Geophys. Res.*, *113*, D12307, doi:10.1029/2007JD009057.

790 Schraner, M., et al. (2008), Technical Note: Chemistry-climate model SOCOL: Version
 791 2.0 with improved transport and chemistry/microphysics schemes, *Atmos. Chem.*
 792 *Phys.*, *8*, 5957–5974, doi:10.5194/acp-8-5957-2008.

793 Scinocca, J. F., N. A. McFarlane, M. Lazare, J. Li, and D. Plummer (2008), Technical
 794 note: The CCCma third generation AGCM and its extension into the middle
 795 atmosphere, *Atmos. Chem. Phys.*, *8*, 7055–7074, doi:10.5194/acp-8-7055-2008.

796 Scinocca, J.F., D.B. Stephenson, T.C. Bailey, and J. Austin (2010), Estimates of past and
 797 future ozone trends from multi-model simulations using a flexible smoothing
 798 spline methodology, *J. Geophys. Res.*, *115*, D00M12,
 799 doi:10.1029/2009/JD013622.

800 Shepherd, T. G. (2008), Dynamics, stratospheric ozone, and climate change, *Atmos.*
 801 *Ocean*, *46*, 117–138, doi:10.3137/ao.460106.

802 Shibata, K., and M. Deushi (2008a), Long-term variations and trends in the simulation of
 803 the middle atmosphere 1980–2004 by the chemistry climate model of the
 804 Meteorological Research Institute, *Ann. Geophys.*, *26*, 1299–1326,
 805 doi:10.5194/angeo-26-1299-2008.

806

807 Shibata, K., and M. Deushi (2008b), Simulation of the stratospheric circulation and ozone
808 during the recent past (1980 – 2004) with the MRI chemistry-climate model,
809 CGER's Supercomp. Monogr. Rep., 14, 154pp., Cent for Gobal Environ. Res.,
810 Natl. Inst. For Environ. Studies, Tsukuba, Japan.

811 SPARC CCMVal (2010), SPARC Report on the Evaluation of Chemistry-Cliamte
812 Models, V. Eyring, T. G. Shepherd, D. W. Waugh (Eds.), SPARC Report No. 5,
813 WcRP-32, WMO/TD-No. 1526.

814 Stolarski, R. S., and A. R. Douglass (1985), Parameterization of the photochemistry of
815 stratospheric ozone including catalytic loss processes, *J. Geophys. Res.*, *90*,
816 10,709-10,718.

817 Stolarski, R. S., and A. R. Douglass (1986), Sensitivity of an atmospheric photochemistry
818 model to chlorine perturbations including consideration of uncertainty
819 propagation, *J. Geophys. Res.*, *91*, 7853-7864.

820 Stolarski, R. S., P. Bloomfield, R. D. McPeters and J. R. Herman (1991), Total Ozone
821 Trends Deduced From Nimbus 7 Toms Data, *Geophys. Res., Lett.*, *6*, 1015-1018.

822 Stolarski, R. S., A. R. Douglass, S. Steenrod, S. Pawson (2006), Trends in stratospheric
823 ozone: lessons learned from a 3D chemical transport model, *J. Atmos. Sci.*, *63*,
824 1028-1041.

825 Stolarski, R. S., A. R. Douglass, P. A. Newman, S. Pawson, M. R. Schoeberl (2009),
826 Relative Contribution of Greenhouse Gases and Ozone-Depleting Substances to
827 Temperature Trends in the Stratosphere: A Chemistry–Climate Model Study, *J.*
828 *Clim.*, *23*, 28-41.

829 Strahan, S. E., et al. (2011), Using transport diagnostics to understand chemistry climate
830 model ozone simulations, *J. Geophys. Res.*, *116*, D17302,
831 doi:10.1029/2010JD015360.

832 Teyssède, H., et al. (2007), A new tropospheric and stratospheric chemistry and
833 transport model MOCAGE-Climat for multi-year studies: Evaluation of the
834 present-day climatology and sensitivity to surface processes, *Atmos. Chem. Phys.*,
835 *7*, 5815–5860, doi:10.5194/acp-7-5815-2007.

836 Tian, W., and M. P. Chipperfield (2005), A new coupled chemistry-climate of the
837 stratosphere: The importance of coupling for future O3-climate predictions, *Q. J.*
838 *R. Meteorol. Soc.*, *131*, 281-303, doi:10.1256/qj.04.05.

839 Tian, W., M. P. Chipperfield, L. J. Gray, and J. M. Zawodny (2006), Quasibiennial
840 oscillation and tracer distributions in a coupled chemistry-climate model, *J.*
841 *Geophys. Res.*, *111*, D20301, doi:10.1029/2005JD006871.

842 Waugh, D. W., and V. Eyring (2008), Quantitative performance metrics for stratospheric-
843 resolving chemistry-climate models, *Atmos. Chem. Phys.*, *8*, 5699-5713.

844 Waugh, D. W., Oman, L., Kawa, S. R., Stolarski, R. S., Pawson S., Douglass, A. R.,
845 Newman, P. A., and Nielsen, J. E. (2009), Impacts of climate change on
846 stratospheric ozone recovery, *Geophys. Res. Lett.*, *36*, L03805,
847 doi:10.1029/2008GL036223.

848 WMO (World Meteorological Organization) (2007), *Scientific assessment of ozone*
849 *depletion: 2006*, Global Ozone Research and Monitoring Project – Report No.
850 50, 572 pp., Geneva, Switzerland.

851

852 WMO (World Meteorological Organization) (2011), *Scientific Assessment of Ozone*
853 *Depletion: 2010: Global Ozone Research and Monitoring Project – Report No.*
854 *52, 516 pp., Geneva, Switzerland.*
855
856
857
858

858 Table 1

Model	Reference
AMTRAC3	<i>Austin and Wilson</i> [2010]
CCSRNIES	<i>Akiyoshi et al.</i> [2009]
CMAM	<i>Scinocca et al.</i> [2008]; <i>de Grandpré et al.</i> [2000]
CNRM-ACM	<i>Déqué</i> [2007]; <i>Teyssiède et al.</i> [2007]
GEOSCCM	<i>Pawson et al.</i> [2008]
LMDZrepro	<i>Jourdain et al.</i> [2008]
MRI	<i>Shibata and Deushi</i> [2008a; 2008b]
Niwa-SOCOL	<i>Schraner et al.</i> [2008]
SOCOL	<i>Schraner et al.</i> [2008]
ULAQ	<i>Pitari et al.</i> [2002]
UMSLIMCAT	<i>Tian and Chipperfield</i> [2005]; <i>Tian et al.</i> [2006]
UMUKCA-METO	<i>Davies et al.</i> [2005]; <i>Morgenstern et al.</i> [2009]
UMUKCA-UCAM	<i>Davies et al.</i> [2005]; <i>Morgenstern et al.</i> [2009]
WACCM	<i>Garcia et al.</i> [2007]

859

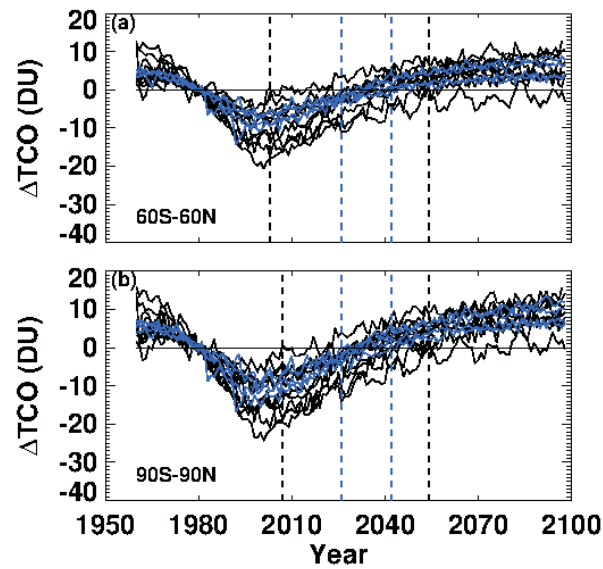
860

860 Table 2

Station	Location
Kiruna, Sweden	67.84°N 20.41° E
Harestua, Norway	60.2°N 10.8 °E
Jungfraujoch, Switzerland	46.55°N 7.98 °E
Kitt Peak, AZ, USA	31.9°N 111.6°W
Izaña (Tenerife), Spain	28.30°N 16.48°W
Mauna Loa, HI, USA	19.54°N 155.58°W
Lauder, New Zealand	45.04°S 169.68°E

861

861 FIGURES



862

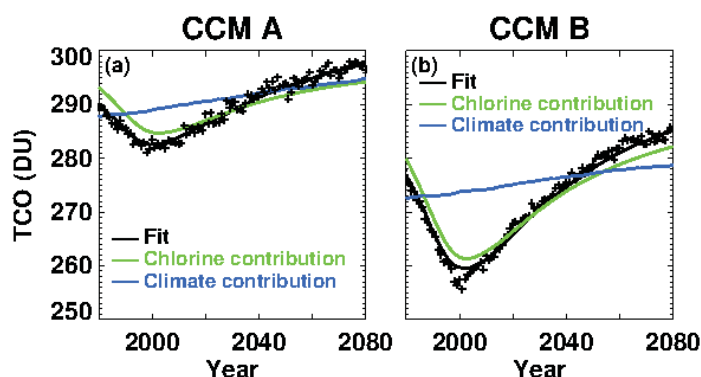
863

864 **Figure 1** a) The difference in the TCO from the 1978-1982 mean for 60°S-60° as
865 simulated by CCMVal models; b) same as a) for 90°S-90°N. In both panels the blue
866 traces identify CCMs with most realistic transport. The dashed black vertical lines
867 indicate the range of years for return to 1980 for the entire group of CCMs; the blue
868 vertical lines indicate the narrower range for the CCMs with most realistic transport.

869

870

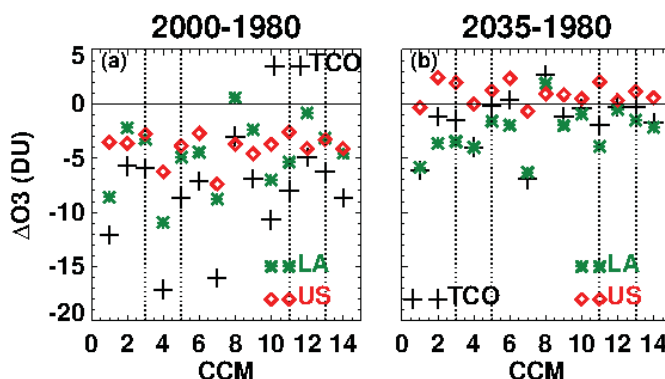
870



871

872 **Figure 2** 60°S-60°N average column ozone from two of the CCMVal CCMs. The
 873 crosses are the annually averaged columns; the black, green and blue lines are the fit
 874 obtained using the MLR, the contribution due to chlorine change and the contribution due
 875 to climate change respectively. The ozone response to climate change is similar for these
 876 examples, but the ozone response to chlorine change differs by more than a factor of 2.

877



878

879

880 **Figure 3** The upper stratosphere and lower atmosphere contributions to the 60°S-60°N
 881 change in TCO between 1980 and 2000 (left) and 1980 and 2035 (right). For both time
 882 intervals, the LA contributes more to the differences in CCM predictions than US. The
 883 dotted vertical lines identify the CCMs with most realistic transport.

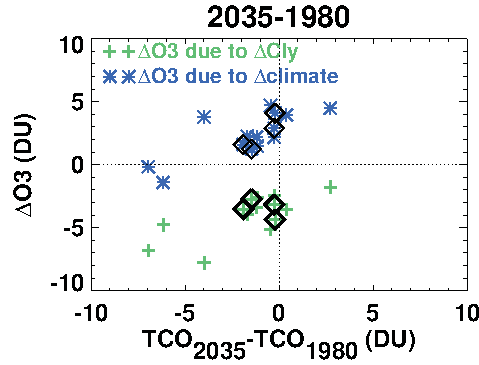


Figure 4 The 2035 – 1980 60°S-60°N contribution due to chlorine change (crosses, y-axis) and that due to climate change (stars, y-axis) as functions of the change in TCO (x-axis). The black symbols indicate the CCMs with most realistic transport.

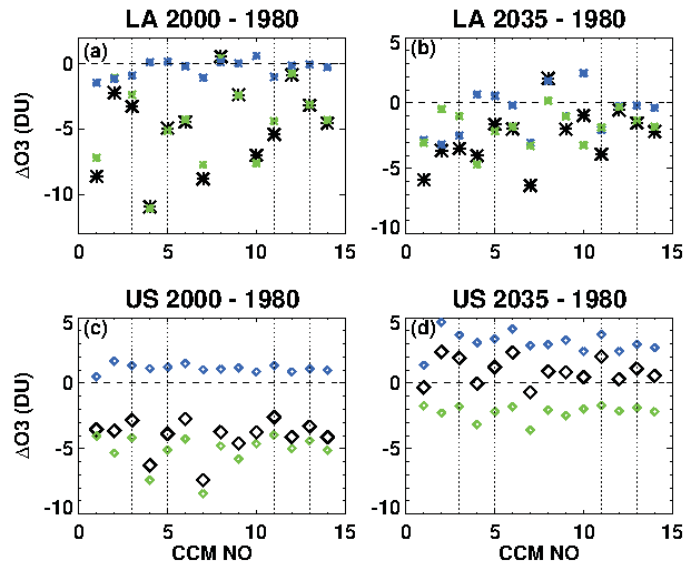
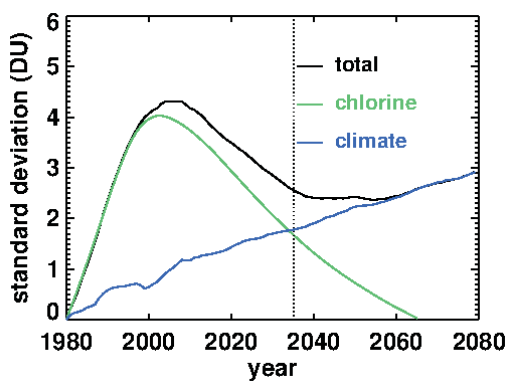


Figure 5 a) The 60°S-60°N LA ozone column change between 2000 and 1980 (crosses), the contribution due to chlorine change (green diamonds), and the contribution due to climate change (blue triangles); b) Same as a) for 2035 and 1980; c) same as a) for the US; d) same as b) for the US. The dotted vertical lines identify the CCMs with most realistic transport.

895



896

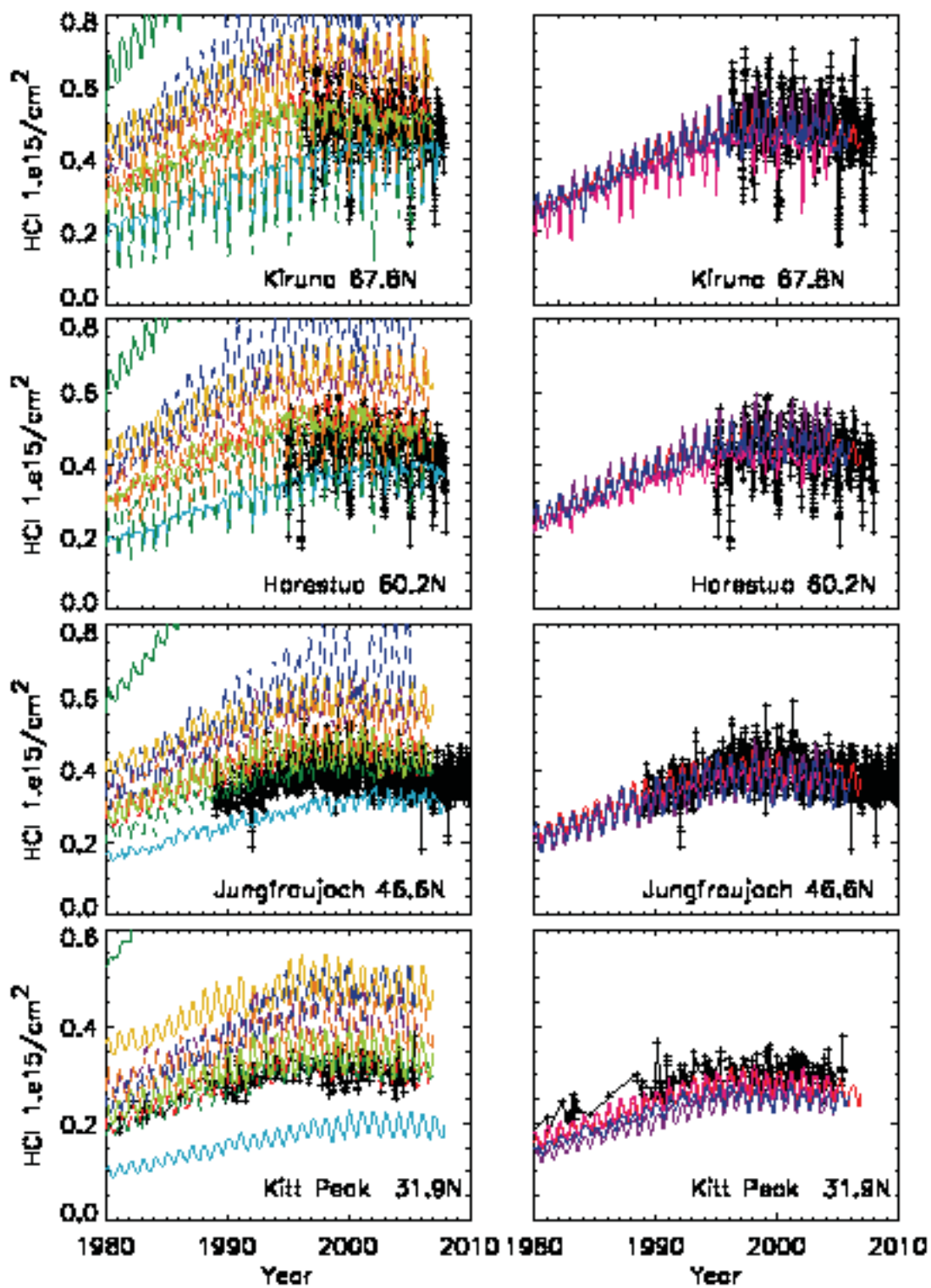
897 **Figure 6** CCM variance for each year between 1980-2080 of the difference from 1980 TCO.

898 The MLR results are used to produce separate time series for the contribution due to chlorine

899 change and the contribution due to climate change. The standard deviations are shown here for

900 the total difference (black), the chlorine contribution (green) and the contribution due to climate

901 change.



902

903

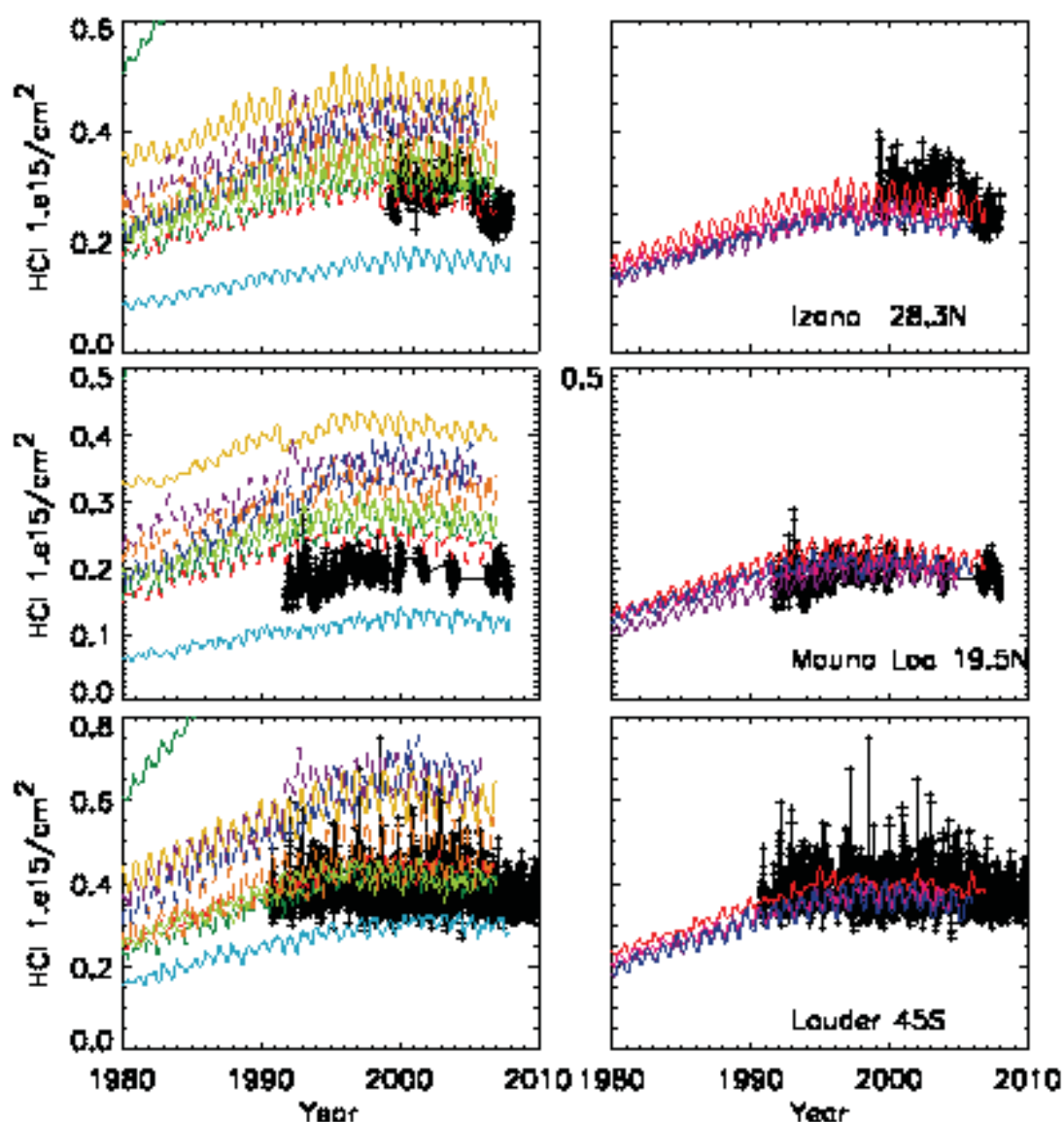


Figure 7 Monthly zonal mean simulated HCl columns at 7 NDACC stations spanning a latitude range $67.8^{\circ}\text{N} - 45^{\circ}\text{S}$ for CCMs with most realistic transport (right column) and for the remaining CCMs (left column). Measurements are overhead columns ($\text{molecules}/\text{cm}^2$).

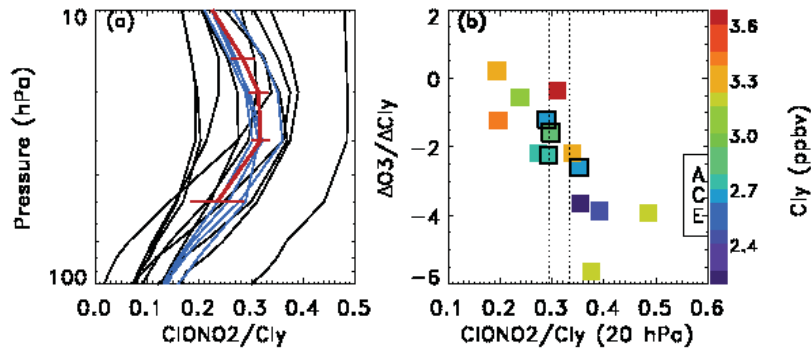
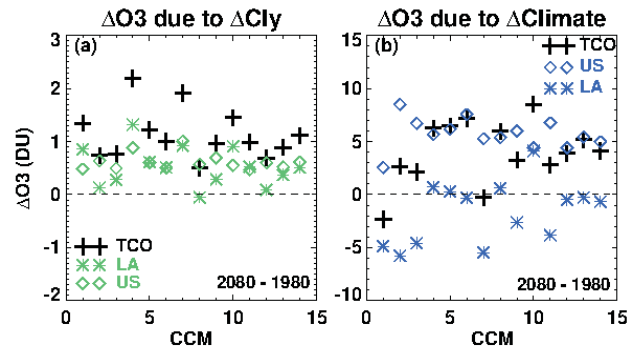


Figure 8 a) The December 2004 mean $\text{ClONO}_2/\text{Cl}_y$ for 45°N from the ACE measurements (red solid line), from the 4 CCMs with most realistic transport (blue solid lines), and from the rest of the CCMs (black solid lines). Horizontal bars on the ACE profile indicate the standard deviation. b) The sensitivity of lower atmosphere ozone to chlorine change ($\Delta O_3/\Delta \text{Cl}_y$) obtained from the MLR as a function of the simulated ratio $\text{ClONO}_2/\text{Cl}_y$ at 20 hPa. The CCMs with most realistic transport are outlined by black squares. Vertical dashed lines indicate the ACE estimate for $\text{ClONO}_2/\text{Cl}_y$ at 20 hPa. The colors of the symbols correspond to the total Cl_y at 20 hPa – the ACE estimate is indicated on the color bar. The correlation coefficient between $\text{ClONO}_2/\text{Cl}_y$ and $\Delta O_3/\Delta \text{Cl}_y$ is -0.78.

920



921

922 **Figure 9** a) ozone change due to chlorine change, 2080 – 1980, upper stratosphere and
 923 lower atmosphere; b) ozone change due to climate change, 2080 – 1980, upper
 924 stratosphere and lower atmosphere.